Re-designing environmentally persistent pharmaceutical pollutant through programmed inactivation: The case of methotrexate

Anaïs Espinosa, Estelle Rascol, Marta Abellán Flos, Charles Skarbek, Pascale Lieben, Eva Bannerman, Alba Diez Martinez, Stéphanie Pethe, Pierre Benoit, Sylvie Nélieu, et al.

▶ **To cite this version:**

Anaïs Espinosa, Estelle Rascol, Marta Abellán Flos, Charles Skarbek, Pascale Lieben, et al.. Re-designing environmentally persistent pharmaceutical pollutant through programmed inactivation: The case of methotrexate. Chemosphere, 2022, 306, pp.135616. 10.1016/j.chemosphere.2022.135616 . hal-03826123

HAL Id: hal-03826123
https://hal.science/hal-03826123

Submitted on 12 Jan 2024

HAL is a multi-disciplinary open access archive for the deposit and dissemination of scientific research documents, whether they are published or not. The documents may come from teaching and research institutions in France or abroad, or from public or private research centers.

L'archive ouverte pluridisciplinaire **HAL**, est destinée au dépôt et à la diffusion de documents scientifiques de niveau recherche, publiés ou non, émanant des établissements d'enseignement et de recherche français ou étrangers, des laboratoires publics ou privés.

Chemosphere 306 (2022) 135616 https://doi.org/10.1016/j.chemosphere.2022.135616

Re-designing Environmentally Persistent Pharmaceutical Pollutant through programmed inactivation: the case of methotrexate

Anaïs Espinosa,[a] Estelle Rascol,[b] Marta Abellán Flos,[b] Charles Skarbek,[b] Pascale Lieben,[c] Eva Bannerman,[b] Alba Diez Martinez,[b] Stéphanie Pethe,[b] Pierre Benoit,[a] Sylvie Nélieu,[a,*] Raphaël Labruère[b,*]

[a] Université Paris-Saclay, INRAE, AgroParisTech, UMR ECOSYS 78850, Thiverval-Grignon, France.
[b] Université Paris-Saclay, CNRS, Institut de chimie moléculaire et des matériaux d'Orsay 91405, Orsay, France.
[c] Université Paris-Saclay, INRAE, AgroParisTech, UMR SayFood 78850, Thiverval-Grignon, France.

Corresponding authors: E-mail: sylvie.nelieu@inrae.fr; E-mail: raphael.labruere@universite-paris-saclay.fr

Keywords: Eco-design • Pharmaceutical pollutants • Photodegradation • Retro catabolic drug design • Structural identification.

Highlights:

- The strategy of "retro catabolic drug design" is disclosed for the programmed/improved inactivation of drugs.
- The drug model is methotrexate and three analogs were synthesized.
- An ether analog displaying similar antitumor activity was selected and its better human metabolic stability was demonstrated.
- Using photo-irradiation, the identified transformation products were mostly obtained from the expected molecular scission.
- A faster kinetics of degradation was measured for the ether analog and its transformation products were less cytotoxic.

Abstract: Environmental emission of pharmaceutical pollutants notably causes the contamination of aquatic ecosystems and drinking water. Typically, reduction of these pollutants in the environment is mostly managed by ameliorated wastewater treatments. Here, we report a method for the eco-design of drugs through the introduction within the molecular structure of a sensitive chemical group responsive to water treatments. The new drugs are thus programmed to fragment more easily and quickly than the original drugs. In this "retro catabolic drug design" strategy, methotrexate was used as drug model and an ether analog displaying a similar pharmacological profile was selected. Using photo-irradiation experiments at 254 nm, a representative drinking water treatment process, the identified transformation products were predominantly obtained from the expected molecular scission. Moreover, a faster kinetics of degradation was measured for the ether analog as compared to methotrexate and its transformation products were far less cytotoxic.

1. Introduction

The presence of Active Pharmaceutical Ingredients (APIs) in the environment has been largely demonstrated, including in soil and soil water,[1-3] in surface water,[4,5] in groundwater[6] potentially used to produce drinking water[7,8] and drinking water itself.[9,10] Current approaches directed at reducing API levels in the environment have focused on pollution control, particularly improved wastewater treatment and take-back collection of unused medications. Even though API manufacturing processes are now greener in term of solvent and energy uses, pharmaceutical companies do not control the entire life cycle of their APIs. K. Kümmerer was the first to propose the better biodegradability in the environment of APIs called the "begnin by design" concept. [11-14] It implies the design of chemicals that will fragment after use in the environment into innocuous and non-persistent transformation products. Recently, β-blockers such as metoprolol and propranolol were subject to a method based on the nontargeted photogeneration of hydroxylated drug analogs since oxygenated compounds were shown to carry better aerobic biodegradability.[15-18] More recently, Kümmerer et al. designed an analog of ciprofloxacin which displayed improved environmental properties in comparison to the parent antibiotic.[19] In addition, photolabile group-containing antimicrobial agents have been succesfully devised to switch off after exposure to light.[20-23]

Herein, we propose to go one step further by implementing a general strategy for the programmable inactivation of drugs. This new approach of "retro catabolic drug design" for the programmed fragmentation of transformation products relies on an inbuilt

sensitive moiety within the ecodesigned drugs. Water treatment processes will trigger the self-disassembly of the oxidized molecule with loss of original activity (Scheme 1).

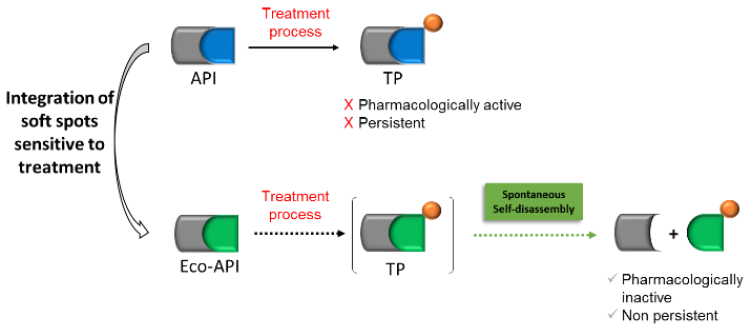

Scheme 1. "Retro catabolic drug design" by integration of water treatment-responsive soft spots into API structures. The original API leads to transformation products (TPs) that can be persistent and still active. Depending on the TPs obtained after a particular treatment process, the newly designed eco-API would bear an easily breakable bond triggered by this treatment. The majority of the new TPs should then undergo facilitated disassembly leading to fragments anticipated as inactive.

The new APIs should be (i) stable toward human metabolism and (ii) soft spots should be incremented at specific molecular positions of the drug candidates. Therefore, these "benign by design" APIs must capitalize on the larger transformation capacity of the treatment processes such as UV treatment compared to the human metabolism. The UV treatment of water is recommended for its strong effectiveness at breaking molecules apart in a short process time.[24] Furthermore, phase I oxidation of human metabolism should be restricted by either its non- or very slow-capacity to oxidize a particular position of an API within its given residence time in the body.

We recently studied the photodegradation of methotrexate (**MTX**),[25] an antimetabolite and antifolate drug in prioritized lists for environmental risk assessment.[26,27] Methotrexate is schematically made of three moieties: a pteridine ring, a *p*-aminobenzoic acid and a glutamic acid (Scheme 2). Upon UV irradiation at both 254 nm and 300-450 nm, we mainly observed the transformation products originating from the fragmentation of the amine bond of methotrexate to afford non-cytotoxic pteridine and aminobenzoyl derivatives (~ 80% at 254 nm and ~ 100% at 300-450 nm).[25] This disassembly can be attributed to well-known mechanisms of either α-oxidation of amines[28,29] or even to self-immolation leading to spontaneous elimination[30,31] (Scheme 2a).

We thus considered methotrexate as a good starting point for the introduction of our approach of eco-designed drugs. In this context, we decided to modify the amine bond within the methotrexate molecule in order to compare the degradability of the new entities with the parent drug. First, we reasoned that the hydrogen abstraction of the C-H bond adjacent to *N*-methyl group would be facilitated by its replacement with a stronger electron withdrawing atom or function during photodegradation. In regards to the self-immolation mechanism, this process would be accelerated by the presence of good leaving groups in contrast to an aniline motif.[30] Thus, three analogs of methotrexate containing either an ether, thioether or carbamate bond between the pteridine nucleus and the benzoyl-glutamyl part were then developed (Scheme 2b). Advantageously, the oxygenated and, to a lesser extent, the thiolated analogs were already shown to display strong anticancer activity *in vitro* and *in vivo*.[32-34]

2. Materials and methods

2.1 Synthesis

The synthesis of the methotrexate analogs is described in the Supporting Information.

2.2. Determination of the IC_{50}s of methotrexate and analogs

The cytotoxicity of the different compounds was tested against A549 cells using a reported procedure.[25] Briefly, 2.5 10^3 cells were seeded and incubated in 96-well plates, and each compound (**MTX**, **OMTX**, **SMTX** and **CarbMTX**) was added at different final concentrations (from 50 µM to 0.05 nM). After 72 h, MTS (Promega) was added in each well and the optical density was measured at 490 nm using a microplate reader (Infinite M200 Pro, Tecan trading AG). Each concentration was tested in six replicates and the experiment was fulfilled in triplicates. The concentration inhibiting 50% of the cell proliferation (IC_{50}) was determined using GraphPad Prism software (GraphPad Software Inc).

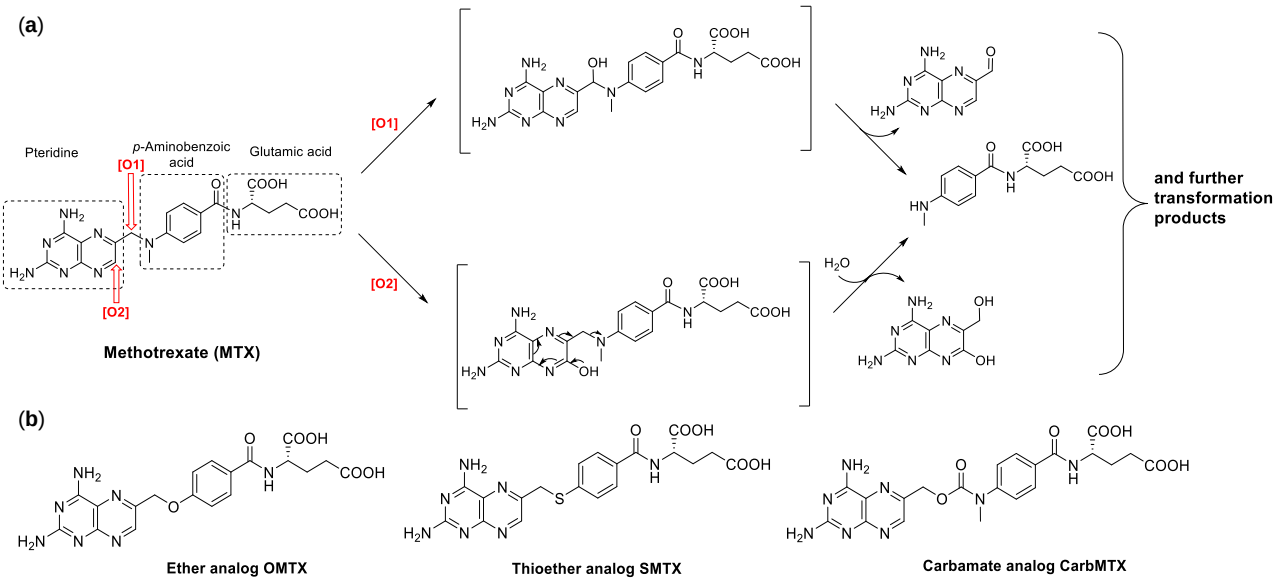

Scheme 2. Structure of methotrexate (**MTX**) and proposed degradation mechanisms by irradiation at 254 nm.[25] Oxidations **[O1]** and **[O2]** are associated to the hydroxylation of the amine bond and the C7 of the pteridine nucleus respectively leading to spontaneous disassembly. (b) Structures of the ether, thioether and carbamate analogs of **MTX** designed to potentially disassemble faster than the parent compound.

2.3. Metabolisation by cytosol from human liver

Methotrexate or analogs solutions (800 µM) were prepared in 10 mM Tris-HCl, pH 7.4 containing 20 mM $MgCl_2$ and 1% DMSO (v/v). Then, 400 µL of the solution containing the compound was mixed with 400 µL of prewarmed human liver cytosol (ThermoFisher Scientific). The mixture was gently shaken at 37 °C and 80 µL of the solution were taken up at different time intervals up to 28 h of reaction. Each sample was filtered (PTFE pore size 0.2 µm) before being analyzed by HPLC.

2.4. Photodegradation

The degradation experiments were carried out as described by Espinosa et al.[25] Briefly, 40 µM solutions of **MTX** or **OMTX**, prepared in Milli-Q water with pH adjusted to pH 7, were exposed either to wavelength conditions representative of natural conditions in surface water (300-450 nm) or drinking water treatment (254 nm). For the 300-450 nm treatment, the solution was placed in a tubular pyrex reactor at the center of a cylindrical device equipped with six lamps emitting within 300 to 450 nm with 365 nm as maximum emission (TLD 15 W, Philips). The temperature was maintained at 20-22 °C by a fan located outside the bottom of the tube. Mixing and oxygenation were assured by air bubbling. For the 254 nm treatment, the solution was placed in a tubular quartz reactor parallel to a monochromatic low-pressure mercury lamp (TUV 15 W, Philips) and mixed by magnetic stirring. At photoreactor location, the light intensity measured by a radiometer (VLX-3W, Vilber Lourmat, Marne-la-Vallée, France) was for each of the six 300-450 nm lamps ca 0.1 mW/cm^2 at 312 nm and 1.2 mW/cm^2 at 365 nm, and with the 254 nm lamp, 1.5 mW/cm^2 at 254 nm.

2.5. Monitoring of photoproducts

The degradation kinetics of the parent compounds (**MTX** and **OMTX**) were established using the HPLC-UV Waters Alliance (2690/5) system on a HPLC C18 Gravity-SB column 150 × 3 mm, 3 µm particle size (Macherey-Nagel) as described by Espinosa et al.[25] A diode-array detector (TUV 2489, Waters) acquiring in the 230-305 nm range was used for detection and data were acquired and treated using Empower software. Peak areas were expressed in percentage of initial **OMTX** (n=4) performed at 290 nm using the 40 µM initial solution as 100% abundance and degradation kinetic was treated as a first order form. Monitoring of TPs were conducted by UHPLC-MS/MS composed by an Acquity UPLC system (Waters) connected to a triple quadrupole mass

spectrometer (TQD, Waters). The acquisitions were performed under MS full scan mode and the quantifications were achieved using the pseudo-molecular ions in positive mode.

2.6. Identification of photoproducts

The structural determination of the transformation products (TPs) was also performed according to Espinosa et al.[25] Briefly, identification was conducted at the end of irradiation and after pre-concentration by solid-phase extraction on Oasis HLB cartridges, with an UHPLC Ultimate 3000 (Thermo Fisher Scientific) coupled to a Q Exactive hybrid quadrupole – Orbitrap™ (Thermo Fisher Scientific) mass spectrometer through a Heated Electrospray Ionization (HESI-II) probe with the same column described above. Full scan within mass-to-charge (*m/z*) range of 120–550 m/z at a mass resolution of 70000 and a scanning speed of 3.7 scan/s was used for acquiring MS data and allowing the detection of the pseudo-molecular ions $[M + H]^+$ and $[M – H]^-$ of the compounds. Higher-energy collisional dissociation (HCD) with a normalized collision energy of 35% was used for the fragmentation of the pseudo-molecular ions and daughter ion were then directed to the Orbitrap and analyzed with a resolution of 35000. Data processing was conducted with Xcalibur™ software (Thermo Fisher Scientific).

3. Results and discussion

We have redesigned the synthesis of the oxygenated analog **OMTX**[32] with several modifications in order to up-scale the synthetic route (Scheme 3). 4-Benzyloxybenzoic acid **1** was coupled to the *tert*-butyl ester-protected glutamate **2** through an amide bond formation using the peptide coupling agent *N*-ethyl-*N′*-(3-dimethylaminopropyl)carbodiimide (EDC) and hydroxybenzotriazol (HOBt). In the second step, removal of the benzyl group of **3** was carried out using hydrogen in presence of palladium on charcoal in excellent yield (98%). The coupling of the pteridine derivative **5** with the previously obtained phenol **4** was performed in dry DMF at room temperature and in the presence of a strong base (NaH). The desired **OMTX** was finally synthesized by the deprotection of the *tert*-butyl groups of **6** with TFA in 90% yield. The preparation of the analogs containing either a thioether or a carbamate bond were prepared following closely related synthetic pathways (Schemes S2 and S3).

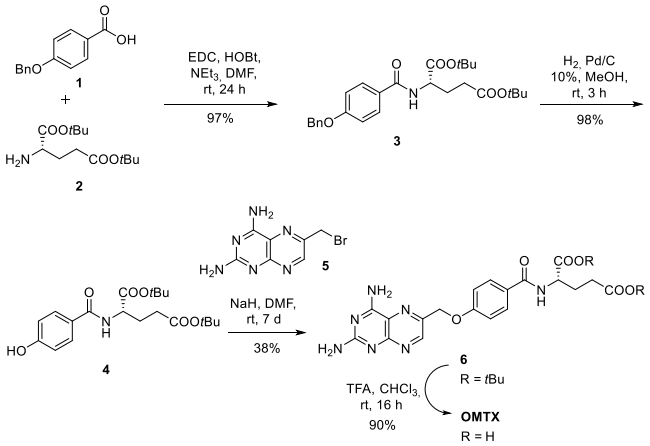

Scheme 3. Synthetic pathway to the ether analog **OMTX**.

In order to evaluate the pharmacological activity of the methotrexate analogs, we first tested their cytotoxic activity against A549 cancer cells. In regards to methotrexate (IC_{50} ~ 0.1 µM), the oxygenated analog **OMTX** exihibited a similar activity (IC_{50} ~ 0.3 µM) and thiolated analog **SMTX** was less cytotoxic (IC_{50} ~ 2.6 µM), in good agreement with the literature. The carbamate analog **CarbMTX** was however completely inactive (IC_{50} > 500 µM) and was not further taken into account.

In vitro hepatic metabolism was then assayed on methotrexate and the bioactive analogs. Methotrexate is subject to liver metabolism with the formation of 7-hydroxymethotrexate under aldehyde oxidase action.[35,36] Using partially purified aldehyde oxidase from rabbit liver,[37,38] the 7-hydroxymethotrexate was obtained as the sole metabolite as expected (Figure S1). We further examined the analogs **OMTX** and **SMTX** and similarly observed the formation of one hydroxylated metabolite of the parent compounds in each case. Then, metabolization of

MTX, **OMTX** and **SMTX** was compared in cytosol from human liver and initial rate of hydroxylation of the different compounds was determined (Figure S2). After 24 h of incubation, 4% of methotrexate was metabolized whereas 7-hydroxymethotrexate was formed at a rate of 1.3 min^{-1}. Under the same conditions, thioether analog **SMTX** was hydroxylated ~ 20 times faster (21.6 min^{-1}) than methotrexate whereas ether analog **OMTX** was slowly converted into the corresponding metabolite (0.06 min^{-1}). From this experiment, we noted that thioether **SMTX** was quickly metabolized up to 34% in 24 h which is detrimental for its potential pharmacological activity as its dose in the organism would hardly reach the effective concentration. However, ether **OMTX** metabolization was slow and we further studied the structure of its metabolite by UHPLC-MS/MS analysis. We concluded that hydroxylation occurred at the 7-position of the pteridine nucleus as in methotrexate (Figures S3-4 and Scheme S4).

Owing to the aforementioned results and since its pharmacological activity was already demonstrated *in vivo*,[34] we then selected the **OMTX** analog for a thorough comparative photodegradation study with methotrexate. Aqueous 40 µM solutions at pH 7 were submitted to irradiation, either at 254 nm or 300-450 nm wavelength; samples were taken regularly and analyzed by HPLC-UV. The aqueous solutions of **MTX** and its analog **OMTX** appeared as stable for at least 24 h in the dark, at pH 7. When irradiated at 300-450 nm, i.e. the wavelength range photoactive in sunlight, the first order kinetic constants of both compounds are of same order of magnitude, 12.8 ± 0.9 10^{-5} s^{-1} and 16.2 ± 0.2 10^{-5} s^{-1} for **MTX** and **OMTX** respectively (Figure S5). The reactivity difference between the two compounds is much more marked when the irradiation was performed at 254 nm, the **OMTX** presenting a first order kinetic constant 32-fold higher than **MTX** (281 ± 4 10^{-5} s^{-1} and 8.8 ± 1.6 10^{-5} s^{-1} for **OMTX** and **MTX**, respectively). Considering the same degradation state (around 20% of residual parent compounds) at this wavelength, this advancement corresponded to only 15 min for **OMTX** whereas 3 h was necessary for **MTX** (Figure 1a). As the process to produce drinking water often includes a 254 nm irradiation step which must be as short as possible in order to avoid the blockage of important volumes of water for a long period, **OMTX** would thus be more efficiently removed than **MTX**.

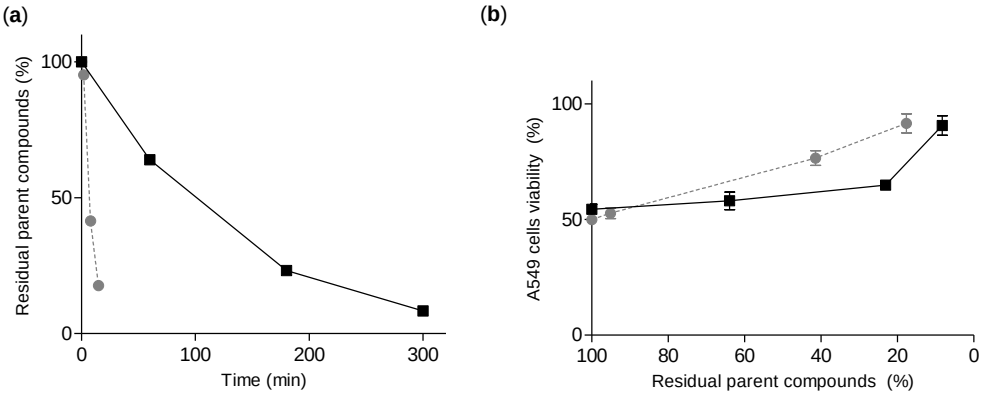

Figure 1. (a) Photodegradation kinetics under 254 nm irradiation of 40 µM aqueous solutions of **MTX** (black squares) and **OMTX** (grey disks). (b) Viability of the A549 cancer cells in function of residual percentage of **MTX** (black squares) and **OMTX** (grey disks) after irradiation at 254 nm.

The structural determinations and the reaction monitoring of the transformation products (TPs) were carried out as described by Espinosa et al.[25] via UHPLC-MS/MS using a high resolution equipment for the identifications and a triple quadripole programmed under multiple reaction monitoring adapted to perform quantitation. The elemental composition of the pseudo-molecular ions and their main fragment ions are summarized in Table S1. Due to the lack of standards corresponding to the hypothesized photoproducts, a comprehensive study of the **OMTX** fragmentation was conducted and presented in Scheme S5. Identifications of a majority of TPs (Schemes 4 and S6) corresponded to a level 2b according to Schymanski et al.[39] Nonetheless, TP267 corresponded to a level 1 as this compound was synthesized and used as chemical standard. TP411a and b, and TP413 coincided to a level 3 because of the lack of stricking information to propose only one structure and finally TP441 to a level 4 due to its similar degradation pathway as **OMTX** which prevented elucidation of its structure. Monitoring of TPs along photodegradation experiments gave indication about mechanisms of degradation (Figure S8). Focusing on

254 nm condition after 3 h of irradiation, 18% of residual **OMTX** were observed and the major photoproducts (> 5%) were TP192, TP441, and also TP208 and TP411b (26%, 15%, 17% and 23% respectively) (Scheme 4 and Table S2). In regards to the expected fragmentation of the ether bond between the pteridine nucleus and the hydroxybenzoyl derivative, we observed that a conversion of ~ 60% with the transformation products TP192, TP206, TP208 and TP267 corresponded to this envisioned scission (Schemes 4 and S6). In regards to the stability of 7-hydroxy metabolites observed in the cytosol, it appears that self-immolation may not be the main mechanism of scission of both **MTX** and **OMTX** upon UV treatment. Therefore, cleavage could mostly occur by direct scission of the ether (**OMTX**) or amine (**MTX**) bond and hydroxylation of the pteridine nucleus would then occur before or after this specified fragmentation. Nonetheless, the UV treatment at 254 nm could also promote self-immolation by the generation of the aryloxy radical (pteridine-O·).[40] Indeed, neither 7-OH-**MTX** nor 7-OH-**OMTX** remained observable at the end of irradiation. Lastly, considering the TPs resulting from modifications of the glutamyl part, the sum was higher for **OMTX** (41%, including TP411a, TP441, TP411b, see Scheme S6 and Table S2) than for **MTX** (30%).[25]

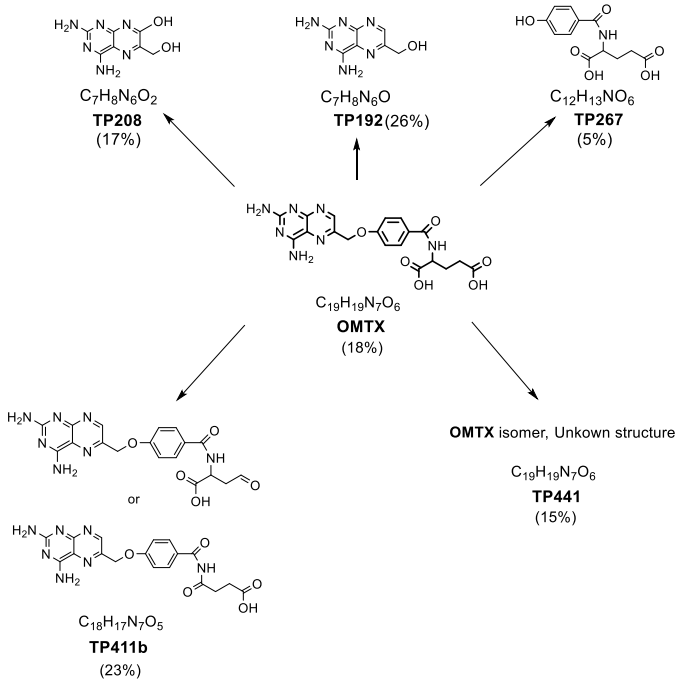

Scheme 4. Proposed structures of the transformation products (> 5%) of **OMTX** under irradiation at 254 nm. Results expressed in % of the initial amount of parent compound and based on relative area as obtained by MS.

Finally, the viability of A549 cancer cells was assessed on all the samples of **OMTX** photodegradation (Figure S6) and compared to the previously described results obtained starting from **MTX**.[21] Only 65% of cell viability was restored after 3 h of **MTX** irradiation whereas the cell viability was almost completely retrieved (~ 90%) in 15 min of **OMTX** irradiation at 254 nm (Figure 1b). At the time point where the amount of residual parent compounds are approximately equivalent: specifically 23% residual **MTX** and 18% residual **OMTX**, the cytotoxicity of the TPs obtained from **OMTX** is greatly weaker than these generated from **MTX** even though the number of TPs generated and identified from **OMTX** (= 9) was higher than that of **MTX** (= 6). Viability evolution under irradiation at 300-450 nm followed a similar trend (Figure S6a).

4. Conclusion

Herein, we have described a methodology for the programmed inactivation of environmentally problematic drugs upon typical water treatment. This strategy relies on the spontaneous disassembly of a dual or multipartite drug triggered by the applied process. The detachments of at least two moieties of the original drug lead to anticipated loss of the pharmacological activity. This last point is crucial since one of the major problems of excreted drugs (or their transformation products) in the environment is essentially the perpetuation of their original biological

activity. Using methotrexate as a drug model, we demonstrated the feasibility of this strategy with the development of a pharmacologically potent analog that is mostly and promptly disassembled by UV treatment into two parts displaying much less cytotoxicity than the parent compound. We have revealed a better photodegradability of the analog compared to methotrexate in a condition representative of the drinking water treatment process. Likewise, several other environmentally problematic drugs of major interest could benefit from a similar re-design. Since the application of this type of wastewater treatment is not available worldwide,[41] it should be noted that the ideal eco-drug should be deactivated as soon as possible after excretion by conditions occurring in the environment (such as photodegradation under sunlight or by biodegradation) and the transformation products generated should also be free of ecotoxicity. As of today, pharmaceutical companies do not survey the persistence of APIs or their metabolites in the environment even though the Food and Drug Administration (FDA) and European Medicines Agency (EMA) request a pre-marketing environmental risk assessment (ERA) before new drug approval. Nonetheless, laws imposing the innocuousness of new APIs toward the environment could be adopted in the future. In the longer term, methods accompanying medicinal chemists to choose compounds that will be harmless to the environment have to be envisioned. Our approach and others emanating from this study could be integrated into the design of new drug candidates.

Credit author statement

Anaïs Espinosa: Data curation, HPLC-MS analysis, Validation, Writing – original draft, Writing – review & editing. Estelle Rascol: Metabolic analysis, Writing – review & editing. Marta Abellán Flos: Chemical synthesis, Writing – review & editing. Charles Skarbek: Cytotoxicity analysis, Writing – review & editing. Pascale Lieben: HPLC-MS analysis, Eva Bannerman: Chemical synthesis. Alba Diez Martinez: Chemical synthesis. Stéphanie Pethe: Sample analysis, Writing – review & editing. Pierre Benoit: Conceptualization, Supervision, Writing – review & editing. Sylvie Nélieu: Conceptualization, Supervision, Funding acquisition, Writing – review & editing. Raphaël Labruère: Conceptualization, Supervision, Funding acquisition, Writing – review & editing.

Acknowledgements

This research is a part of the EDIFIS project funded by a grant from the French National Agency for Research (ANR-16-CE34-0001-01). The research was also supported by grants from INRAE (AgroEcoSystem division) and the French ministry of Agriculture and Food for AE PhD scholarships. The authors are grateful to Laure Moreau and Maïlys Bagnères for their assistance in synthetic chemistry. We also acknowledge Hatouma Traoré and Edwige Kouadio for their work on the initial analytical developments and to Brigitte Pollet for her help on exact mass analysis.

References

[1] M. Edwards, E. Topp, C. D. Metcalfe, H. Li, N. Gottschall, P. Bolton, W. Curnoe, M. Payne, A. Beck, S. Kleywegt, D. R. Lapen, *Sci. Total Environ*. **2009**, *407*, 4220-4230.

[2] C. Wu, A. L. Spongberg, J. D. Witter, M. Fang, K. P. Czajkowski, A. Ames, *Arch. Environ. Contam. Toxicol*. **2010**, *59*, 343-351.

[3] N. Gottschall, E. Topp, C. Metcalfe, M. Edwards, M. Payne, S. Kleywegt, P. Russell, D. R. Lapen. *Chemosphere* **2012**, *87*, 194-203.

[4] T. L. ter Laak, M. van der Aa, C. J. Houtman, P. G. Stoks, A. P. van Wezel, *Environ. Internat*. **2010**, *36*, 403-409.

[5] S. R. Hughes, P. Kay, L. E. Brown, *Environ. Sci. Technol*. **2013**, *47*, 661-677.

[6] B. Lopez, P. Ollivier, A. Togola, N. Baran, J. P. Ghestem, *Sci. Total Environ.* **2015**, *518-519*, 562-573.

[7] M. J. Benotti, R. A. Trenholm, B. J. Vanderford, J. C. Holady, B. D. Stanford, S. A. Snyder, *Environ. Sci. Technol.* **2009**, *43*, 597-603.

[8] M. S. Fram, K. Belitz, *Sci. Tot. Environ*. **2011**, *409*, 3409-3417.

[9] J. Fick, H. Söderström, R. H. Lindberg, C. Phan, M. Tysklind, J. D. G. Larsson, *Environ. Toxicol. Chem.* **2009**, *28*, 2522-2527.

[10] E. Vulliet, C. Cren-Olivé, M. F. Grenier-Loustalot, *Environ. Chem. Lett*. **2009**, *9*, 103-114.

[11] K. Kümmerer, *Green Chem.* **2007**, *9*, 899-907.

[12] K. Kümmerer, D. D. Dionysiou, O. Olsson, D. Fatta-Kassinos, *Science* **2018**, *361*, 222-224.
[13] K. Kümmerer, *Angew. Chem. Int. Ed.* **2017**, *56*, 16420-16421.
[14] K. Kümmerer, *Sustain. Chem. Pharm.* **2019**, *12*, 100136.
[15] T. Rastogi, C. Leder, K. Kümmerer, *Chemosphere* **2014**, *111*, 493-499.
[16] C. Leder, T. Rastogi, K. Kümmerer, *Sustain. Chem. Pharm.* **2015**, *2*, 31-36.
[17] T. Rastogi, C. Leder, K. Kümmerer, *Environ. Sci. Technol.* **2015**, *49*, 11756-11763.
[18] T. Rastogi, C. Leder, K. Kümmerer, *RSC Adv.* **2015**, *5*, 27-32.
[19] C. Leder, M. Suk, S. Lorenz, T. Rastogi, C. Peifer, M. Kietzmann, D. Jonas, M. Buck, A. Pahl, K. Kümmerer, *ACS Sustainable Chem. Eng.* **2021**, *9*, 9358-9368.
[20] W. Lee, Z.-H. Li, S. Vakulenko, S. Mobashery, *J. Med. Chem.* **2000**, *43*, 128-132.
[21] W. A. Velema, J.-P. van der Berg, M. J. Hansen, W. Szymanski, A. J. M. Driessen, B. L. Feringa, *Nat. Chem.* **2013**, *5*, 924-928.
[22] S. Hubick, A. Jayaraman, A. McKeen, S. Reid, J. Alcorn, J. Stavrinides, B. T. Sterenberg, *Sci. Rep.* **2017**, *7*, 41999.
[23] V. Eikemo, L. K. Sydnes, M. O. Sydnes, *RSC Adv.* **2021**, *11*, 32339-32345.
[24] I. Kim, H. Tanaka. *Environ. Int.* **2009**, *35*, 793-802.
[25] A. Espinosa, S. Nélieu, P. Lieben, C. Skarbek, R. Labruère, P. Benoit, *Environ. Sci. Pollut. Res. Int.* **2022**, *29*, 6060-6071.
[26] J. P. Besse, J. F. Latour, J. Garric, *Environ. Internat*. **2012**, *39*, 73-86.
[27] V. Booker, C. Halsall, N. Llewellyn, A. Johnson, R. Williams, *Sci. Tot. Environ*. **2014**, *473-474*, 159-170.
[28] M. Largeron, *Eur. J. Org. Chem.* **2013**, *2013*, 5225-5235.
[29] N. Karpel Vel Leitner, P. Berger, B. Legube. *Environ. Sci. Technol.* **2002**, *36*, 3083-3089.
[30] A. Alouane, R. Labruère, T. Le Saux, F. Schmidt, L. Jullien, *Angew. Chem. Int. Ed.* **2015**, *54*, 7492-7509.
[31] M. E. Roth, O. Green, S. Gnaim, D. Shabat, *Chem. Rev.* **2016**, *116*, 1309-1352.
[32] J. A. Montgomery, J. R. Piper, R. D. Elliott, C. Temple Jr, E. C. Roberts, Y. F. Shealy, *J. Med. Chem.* **1979**, *22*, 862-868.
[33] F. M. Sirotnak, P. L. Chello, D. M. Moccio, J. R. Piper, J. A. Montgomery, J. C. Parham, *Biochem. Pharmacol.* **1980**, *29*, 3293-3298.
[34] M. G. Nair, T. W. Bridges, T. J. Henkel, R. L. Kisliuk, Y. Gaumont, F. M. Sirotnak, *J. Med. Chem.* **1981**, *24*, 1068-1073.
[35] H. Breithaupt, E. Küenzlen, *Cancer Treat. Rep.* **1982**, *66*, 1733-1741.
[36] A. Moriyasu, K. Sugihara, K. Nakatani, S. Ohta, S. Kitamura, *Drug Metab. Pharmacokinet.* **2006**, *21*, 485-491.
[37] D. G. Johns, A. T. Iannotti, A. C. Sartorelli, J. R. Bertino. *Biochem. Pharmacol.* **1966**, *15*, 555-561.
[38] D. G. Johns, T. L. Loo. *J. Pharm. Sci.* **1967**, *56*, 356-359.
[39] E. L. Schymanski, J. Jeon, R. Gulde, K. Fenner, M. Ruff, H. P. Singer, J. Hollender, *Environ. Sci. Technol.* **2014**, *48*, 2097–2098.
[40] S. Zhao, H. Ma, M. Wang, C. Cao, J. Xiong, Y. Xuc, S. Yao, *Photochem. Photobiol. Sci.* **2010**, *9*, 710-715.
[41] United Nations Habitat and WHO, Annual Report 2021, HS/001/22E, available from https://unhabitat.org/annual-report-2021.